Designing and Prototyping a 3D Printer for Multi-Extrusion of Thermo- and Photocurable Hydrogels: Enabling Affordable and Wider Access to Bioprinting

Afonso Gusmão[1,2,3] · Diana M. C. Marques[1,2] · Rodrigo Torres-Garcia[1,2] · Frederico Castelo Ferreira[1,2,*] · Paola Sanjuan-Alberte[1,2,*] · Marco Leite[3,*]

[1] Department of Bioengineering and Institute for Bioengineering and Biosciences, Instituto Superior Técnico, Universidade de Lisboa, Av. Rovisco Pais, 1049-001, Lisbon, Portugal

[2] Associate Laboratory i4HB – Institute for Health and Bioeconomy, Instituto Superior Técnico, Universidade de Lisboa, Av. Rovisco Pais, 1049-001, Lisbon, Portugal

[3] IDMEC, Instituto Superior Técnico, Universidade de Lisboa, Av. Rovisco Pais, 1049-001, Lisbon, Portugal

*Corresponding authors: frederico.ferreira@tecnico.ulisboa.pt, paola.alberte@tecnico.ulisboa.pt, marcoleite@tecnico.ulisboa.pt

Abstract

3D bioprinting is an area expanding rapidly, allowing for the design of intricate structures using multiple materials, including living cells. This has enormous potential for applications in drug testing, regenerative medicine, and more recently with the surge of the alternative protein field, cell-based food products. Therefore, strategies to effectively implement 3D bioprinting approaches are highly desirable. However, the high cost of equipment is a significant limitation for implementing these approaches. In this work, we aim at designing and developing a low-cost 3D extrusion bioprinter that allows for a wider access to this technique while presenting an extensive range of features compatible with multiple biomaterials. Initially, a fused deposition modelling (FDM) desktop 3D printer (Ender 3-V2) was modified and the mainboard and electronics were reconfigured to host two printing nozzles in the printhead. The designed extrusion system presented a maximum output force of 320 N and featured a temperature control unit (in the range of 2-50^{o}C) and UV-LEDs. Furthermore, this prototype was compatible and fully controlled with open-access software. The printability of the prototype was subsequently evaluated, consisting on a Pr of 0.995, being comparable with commercial solutions. The printer accuracy and precision were also assessed by developing representative calibration models based on ISO guidelines at various temperatures, deposition rates, dispensing tips and printing parameters; presenting high precision and low dimensional errors. Finally, to demonstrate its compatibility with the bioprinting process, we also successfully bioprinted scaffolds containing L929 mouse fibroblasts, maintaining a 97% cell viability seven days after post-printing. This work presents a prototype that integrates a greater number of features and functionalities than other low-cost bioprinters, offering one of the best price-quality ratios. As a result, this technology has the potential to positively impact the field by improving accessibility for users and facilitating its further expansion.

Keywords 3D Extrusion Bioprinting; Low-cost Design for AM; Natural Bioinks; Thermal Crosslinking; Photo Crosslinking

1 Introduction

Due to an increasing world population and life expectancy, the number of patients requiring organ transplantation is increasing [1,2]. As a result, tissue engineering (TE) is a rapidly expanding seeking to repair, replace, or regenerate living tissues or organs by combining knowledge cell biology, materials science, and many aspects of biomedical engineering [3]. Over the last decade, three dimensional (3D) bioprinting has grown from a niche research area to a pillar of TE [4]. Besides the applications in TE, bioprinting technology can also be applied in the new field of alternative proteins, namely cellular agriculture, which aims to engineer animal tissues in vitro for human consumption [5, 6].

Figure 1: Schematic depicting various extrusion bioprinting modalities. (a) Extrusion-based Bioprinting (EBB) results from the continuous extrusion of biomaterials and cells onto a specific substrate through a pneumatic or mechanical system, such as a piston or a screw. Resolution is in the order of 200 µm, and a narrow range of viscosities can be used [7]. **(b)** Freeform

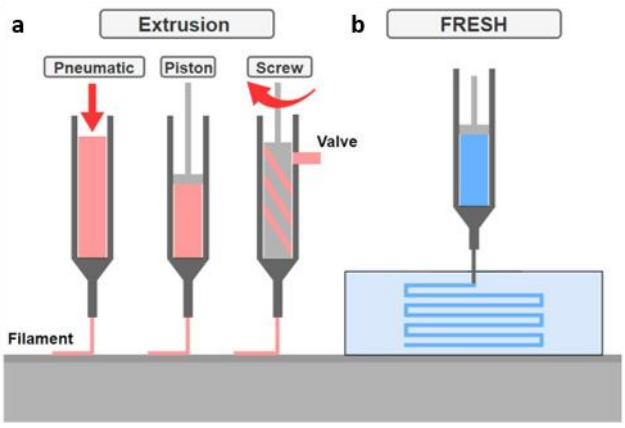

reversible embedding of suspended hydrogels (FRESH) 3D bioprinting into a gelatine microparticle bath.

The most commonly used bioprinting technique is extrusion-based bioprinting (EBB) (**Figure 1a**) due to its excellent deposition rate, flexibility, affordability, and compatibility with multiple bioinks and cell types to produce functional tissues in vitro [4,8]. Another EBB modality consists on the freeform reversible embedding of suspended hydrogels (FRESH) where the biomaterial is extruded from a syringe into a support bath to preserve their mechanical stability during the printing process as shown in **Figure 1b** [9,10]**.** Examples of bioprinted structures manufactured by EBB include functional skin and cartilage [11], branched vascular trees [12], aortic valves [13], *in vitro* pharmacokinetic platforms [14], and tumour models [15], among many others [4].

Currently, commercially available bioprinters are highly precise, but also specific, and restricted equipment. Examples of commercial bioprinters considered low-cost are BIO X, Allevi 1, BIOCOT, INKREDIBLE, STEMAKER GEG4LIFE, and AXO A1-A6 [16]. However, some can exceed 50 000 EUR, which might be considered unaffordable to low-budgeted laboratories and research groups. These printers are microextrusion-based, and most are pneumatically controlled [16,17]. Besides the high cost of these devices, they present very little flexibility in their modification. In addition, they require large quantities of bioinks, often consisting on costly natural polymers and optimized for proprietary and expensive bioink's formulations.

In order to progress and expand this research area, many research groups designed and manufactured low-cost and open-source extrusion bioprinters in house as shown in **Table 1** as an alternative to the commercial options. Some of the most complete prototypes include the Modification of Prusa i3 MK3 performed by members of the Lulea University featuring two extruders and a UV curing system [18] or the EFL-BP6601 and EFL-BP5800 developed at the Zhejiang University, consisting on one extruder with ultra-low resolution (3 µm) and temperature control in the range of 5-37°C [19] among others. However, none of these low-cost options is able to incorporate temperature control and UV curing on two independent extruders for multi-material deposition on the same equipment.

Therefore, this work aims at designing and developing a low-cost 3D extrusion bioprinter that integrates temperature control and UV curing on two independent extruders to increase the adaptability of the bioprinter to different biomaterials. The development of low-cost bioprinting equipment has the potential to reach multiple professionals in both public and private sectors, making access to this technology more affordable, customisable and universal, which might have a direct impact on the TE field.

2 Methodology

2.1 Low-cost Bioprinter Design & Development

The manufacturing phase of this project took place in the Lab2Prod of Instituto Superior Tecnico, Lisbon (Portugal) specialising in Additive Manufacturing, and most of the parts of the working prototype were 3D printed in an Ultimaker S5 (Ultimaker B.V., Utrecht, Nederland). Despite the effort to reuse the printer's original components, many of the components relating to the bioink's temperature control, extrusion and UV curing were obtained from third parties, with a total cost of 735.56 EUR, as can be seen in **Table S1**. It was also required to solder electrical connections and machine some parts to obtain the final prototype.

Table 1: Low-cost extrusion-based bioprinters and their specifications developed by research groups.

Bioprinter	Extrusion Mechanism	Number of Nozzles	Temperature Control	UV Curing	Maximum Resolution	University/ Company	
Multihead Deposition System (MHDS)	Screw-Driven	Four (Synthetic polymers and non-synthetic including hydrogels)	None	None	200 µm	Pohang University of Science and Technology (POSTECH)	[20]
Modification of MakerBot Replicator	Screw-Driven	Two (hydrogels)	None	None	50 µm	Carnegie Mellon University, Pittsburgh, PA, USA	[9]
Modification of Felix 3.0	Screw-Driven	One (hydrogels)	None	None	13 µm (*x* and *y* axes) 0.39 µm (*z* axis)	Old Domonion University, Norfolk, VA	[21]
Replistruder 4	Screw-Driven	One (hydrogels)	None	None	50 µm	Carnegie Mellon University, Pittsburgh, PA, USA	[22]
Modification of E3D tool changer and motion system	Screw Driven	Up to Four, with tool changer (hydrogels)	None	None	50 µm	Uppsala University, Uppsala, Sweden	[23]
Modification of Prusa i3 MK3	Screw-Driven	Two (synthetic polymers and hydrogels)	None	Yes (UV LED 365 nm)	300 µm (*x* and *y* axis) 100 µm (*z* axes)	Lulea University of Technology, Lulea, Sweden	[18]
EFL-BP6601 and EFL-BP5800: Academically developed, but available commercially	Pneumatic-Driven	One (hydrogels)	Yes (5-37ºC)	None	3 µm	Zhejiang University, Hangzhou, China	[19]
Multi-arm Bioprinter (MABP)	Pneumatic-Driven	Three (hydrogels and cell spheroids)	None	None	16 µm	The University of Iowa City, Iowa City, IA, USA	[24]
Large Volume Extruder (LVE)	Screw-Driven	One (hydrogels)	None	None	200 µm	Carnegie Mellon University, Pittsburgh, PA, USA	[25]
Nydus One Syringe Extruder (NOSE)	Screw-Driven	One (hydrogels)	None	None	300 µm (*x* and *y* axis) 100 (*z* axes)	Ruhr University Bochum, Universitatsstrasse, Bochum, Germany & University Medical Centre Utrecht, Uppsalalaan, Utrecht, Germany	[26]
Palmetto 3D bioprinter	Pneumatic-Driven	One (hydrogels)	None	None	10 µm	Medical University of South Carolina and Clemson University	[27]

						and assembled by Izumi International (Greenville, SC), USA	
Modification of 3D Anet A8 Prusa i3 Kit	Screw-Driven	One (hydrogels)	None	None	100 µm	Friedrich-Alexander-University Erlangen-Nürnberg, Erlangen, Germany	[28]
Modification of Witbox2	Pneumatic Driven	One (hydrogels)	Yes (2-60ºC)	None	20 µm	University of Helsinki, Filand; Tkyo Women's Medical University, Japan; University of La Rioja, Logroño, Spain	[29]
Ystruder (with sensing and motion capabilities	Screw Driven	One (hydrogels)	None	None	100 µm	Aalto University, Espoo, Filand; Michigan Technology University, Houghton, MI, USA	[30]

2.1.1 Specifications and Low-Cost 3D Printer Modifications

A FDM-type Creality Ender-3 V2 3D printer (Creality, Shenzhen, China) was utilized as chassis and modified to obtain the 3D extrusion bioprinter prototype. This printer was purchased as a kit and after its assembly, was tested to check if any axle was warped. This printer uses a Cartesian dimensional coordinate system, in which the printhead moves along the XZ vertical plane, whereas the printing bed moves along the XY horizontal plane, and has a build capacity of 220 × 220 × 250 mm. The X and Y axes are moved by pulleys and sprockets, while a lead screw offers the Z axis movement. The dimensional accuracy of this printer is about 100 µm.

For the printer to have two extruders in the printhead, the printer's electronics were reconfigured, including its mainboard. The printers' open-source electronics included an Arduino microcontroller built on the ATmega2560 platform (Mega 2560rev3, Arduino.cc, Turin Italy) and a RepRap Arduino Mega Polulu Shield v1.4 (RAMPS 1.4, Ultimachine, South Pittsburg, TN, U.S.) connected to a 12 Vdc/ 10 A power supply. In the RAMPS v1.4, DRV8825 (Pololu Corporation, Las Vegas, NV, U.S.) stepper drivers were installed. These drivers have mode pins that enable the configuration of the motor up to 1/32 steps per pulse, increasing the smoothness of torque delivery, low-speed motion, and resonance improvement. They can drive up to 2.5 A to each output (with proper heatsinking).

The bioprinter firmware was written in C++, specifically in Marlin (v2.0, https://marlinfw.org/).

2.1.2 Printhead Design and Manufacture

The printing cartridges used in this project were made of polypropylene and have a volume of 3 mL (Nordson EFD Optimum, Westlake, OH, U.S.). The design of the printhead was based around the dimensions of these printing cartridges, which have an outer diameter of 11.1 mm. Figure 2 shows a detailed view of the printhead, using SolidWorks (Dassault Systèmes SolidWorks Corporation, Waltham, MA, U.S.) as CAD software where it can be seen all the components, including the bioink depositing system (**Figure 2a**) and the Peltier-based temperature control system (**Figure 2b**). The temperature control mechanism is formed by an aluminium block, machined to have the desired dimensions (LTO, Instituto Superior Tecnico, Lisbon, Portugal), and a Peltier thermoelectric module (TEC1-12705, Transfer Multisort Elektronik Sp., Łódź, Poland) fixed in the aluminium block to control the heating/cooling of the syringe. On the opposite side of the aluminium block, a heat sink in black anodised aluminium (012-0053, Robert Mauser Lda, Lisbon, Portugal) was placed, which allows cooling the Peltier in case of heating, making the system more efficient.

Printhead parts were manufactured by 3D FDM using an Ultimaker S5 with a build volume of 330 × 240 × 300 mm. This 3D FDM printer was used due to its low cost and good technical specifications, namely a layer resolution of 0.4 mm and a maximum build speed of 24 mm s^{-1}. The material used to manufacture the 3D printed parts was polyethylene terephthalate glycol (PETG), due to its excellent mechanical properties, ease of printing, price-quality ratio, and availability. A layer height of 0.2 mm and infill density of 35% was recommended and used, as seen in **Table S2**, where the main printing parameters are specified. The printhead support has a fundamental and structural role in the entire operation. As it can be seen in **Figure 2c**, this printhead support has many cavities, so polyvinyl alcohol (PVA) was used as a support material during the manufacture of this piece to ensure that it was built without presenting any distortion. PVA is soluble in water and at the end of the 3D FDM job, the part was washed in water for a couple of hours.

An aluminium block, as seen in **Figure S1**, was designed to contain a hole, where an EPCOS 100K thermistor (TDK Electronics AG, Munich, Germany) was placed to measure the system's temperature on the syringe side. The linear actuation of the deposition system was induced with a non-captive stepper motor (Nema 17SL19, OMC, Jiangning, China), which contained a pitch of 2 mm and a holding torque of 0.44 Nm, at a rated current of 1.68 A. A rails system has been designed to constrain the rotational movement of the lead screw, obtaining a linear movement. These rails were 3D printed by FDM. It is important to mention that the custom-built deposition system designed in this project is similar to other solutions in the literature [22]. All these elements were wrapped in a 3D-printed shell (**Figure 2d**) and then assembled on the printhead.

2.1.3 Thermal Control of the Printhead

The temperature control system was divided into two main parts: the temperature detection unit and the Peltier power control unit **Figure 2e**. A NTC 100k thermistor and a voltage divider circuit were used to detect the printing cartridge's temperature. Moreover, a RC (Resistor-Capacitor) low-pass filter (**Figure S2**) was used with a resistance of 47 kΩ and a 10 µF capacitor, to obtain a cut-off frequency of 0.3386 Hz. The application of the filter prevented significant oscillations/noise in thermistor readings, which could later result in false readings and, thus, false inputs for the calculation of the Peltier modules controller. The main components for the temperature control unit were an Arduino microcontroller with a PID control implemented, a difference amplifier circuit, a digital to analogue circuit (DAC), and a power amplifier circuit. This approach has been implemented since the microcontroller has output signals between 0 V and the Vcc voltage, i.e., the maximum Arduino voltage output. In the case of Arduino components, the available values for Vcc are typically 3.3 V or 5 V. Peltier modules, for their regular operation, need higher voltage than 5 V. To obtain analogue outputs, the Arduino use the technique of Pulse Width Modulation (PWM), which consists of obtaining analogue results with digital means. Thus, the mean power offered by an electrical signal can be modelled by chopping it into discrete parts. The length of time the signal is on and off is called the pulse width. Thus, the analogWrite() function was presented on a scale of 0 to 255, such that analogWrite(255) requests 100% duty cycle always on, analogWrite(127) requests 50% duty cycle always on and so on. The Arduino output signals were based on the user's input temperature and the readings obtained by the thermistor. The DAC and difference amplifier were used to convert the eight bits output from the microcontroller to an analogue signal ranging from -12 V to +12 V. The control

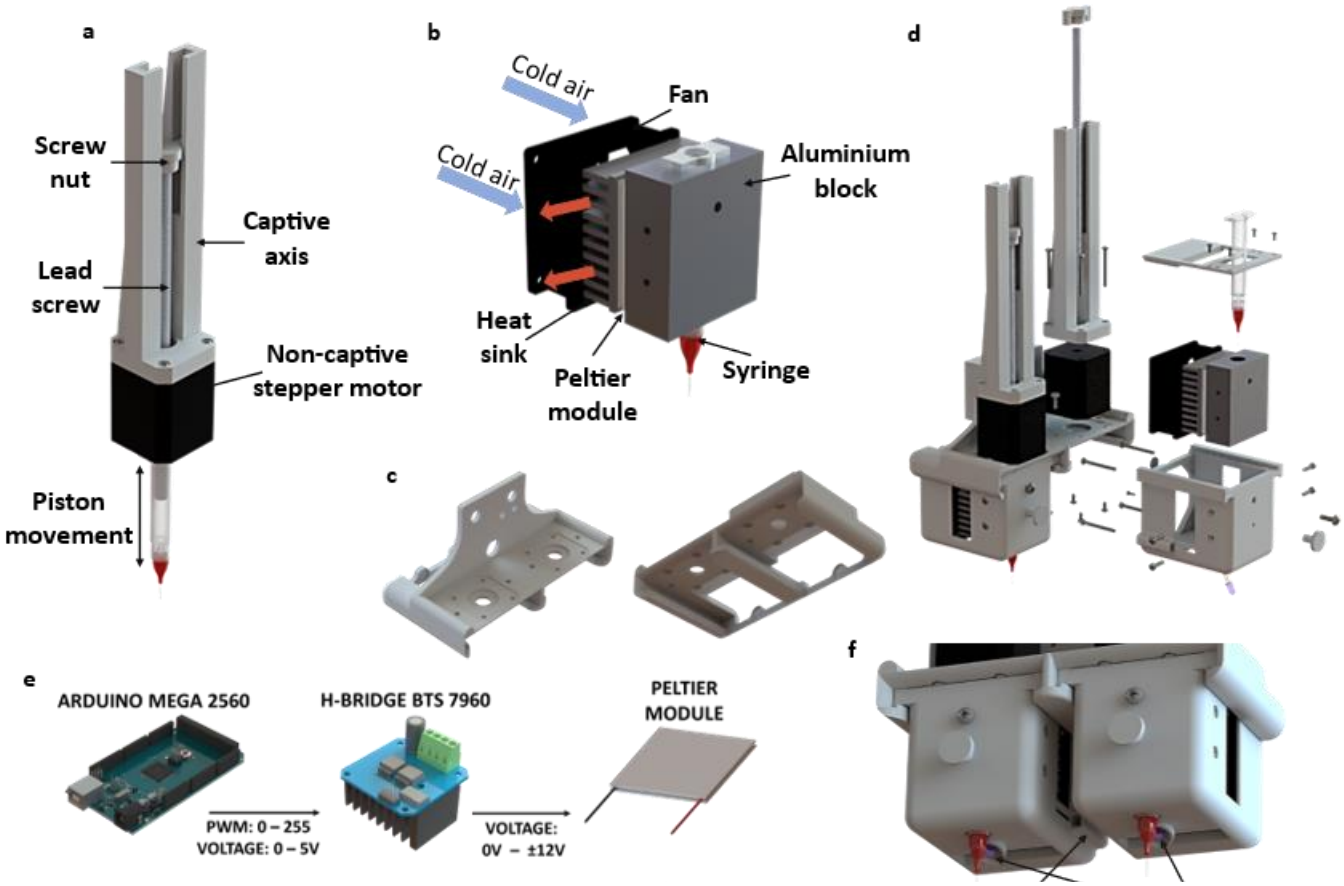

Figure 2: Design of the printhead. **(a)** Isometric view of CAD illustrations of the syringe pump mechanism. The linear movement of the screw is obtained by two 3D-printed parts: (i) the captive rail, which guides the lead screw according to its axis, and; (ii) the screw nut, which is inserted at the opposite end to the lead screw syringe, constraining its rotational movement. **(b)** Temperature control unit designed and integrated into the extrusion head of the 3D bioprinter. The blue and red arrows represent the principle of operation for printhead cooling. **(c)** Printhead support. This component is responsible for fixing the cooling unit and the extrusion mechanism to the rest of the Ender-3 V2 structure. **(d)** Exploded view of the printhead. As can be seen, it contains two extruders, which allow printing with two bioinks simultaneously. **(e)** The prototype's circuit apparatus that regulates the Peltier modules' supply voltage and invert their polarity to obtain a cooling or heating syringe temperature control. **(f)** UV LED curing system present at the 3D bioprinter prototype.

unit run the PID control algorithm inside the microcontroller and, at each given moment, an outputs control signal was generated, considering the temperature detected by the thermistor and the target temperature set point. As mentioned above, the microcontroller's output went through a digital to analogue converter (DAC), then a power amplifier and lastly was sent to the Peltier module. Consequently, the output signal from the microcontroller had enough power to drive the Peltier to heat or cool.

The BTS7960 43 A h-bridge (43 A High Power BTS7960 DC Motor Driver Module, Handson Technology Enterprise, Johor, Malaysia) is a module that allows controlling the circuit supply voltage up to 24 V through a PWM signal. These modules contain 8 Arduino pins, 6 of which are digital, 2 of which are PWM, which must be connected to PWM PIN Arduino. These two RPWM (right direction) and LPWM (left direction) pins allowed regulating the voltage that supplied the load, and for cooling the RPWM pin was used as input. Finally, a liquid crystal display (LCD) (Handson Technology Enterprise, Johor, Malaysia) showed live the temperatures of each printing cartridge. The LCD prompted a message when the aluminium block reached the set temperature.

2.1.4 UV Curing

UV LEDs were positioned on the side of the cartridge's cavity, with its focus directed towards the metal tip end of the needles, as seen in **Figure 2f**. Two 365 nm 5V LEDs (LED, Jiatong, China) were added. The chosen configuration enabled UV curing during printing or in between layers. Two PWM pins were used to connect the LED to the RAMPS 1.4 Arduino shield, allowing it to control the supply voltage from 0 to 5 V and turn it on and off.

2.1.5 Toolpath and Thermal Input: Software Requirements and Sourcing

All the models printed and presented in this work were modelled using CAD software (SolidWorks). The toolpath generation software (Ultimaker Cura v5.0, Ultimaker B.V., Utrecht, Nederland) was used to generate the various G-code files containing all the movement and deposition commands that the printer must have during the printing process. In the case of structures with several layers of material, the spacing between them was equal to the internal diameter of the needle used to obtain a uniform filament whose thickness was equal to its height. To activate the UV LEDs during the printing process, G-CODE lines referring to turning on and off pins 6 and 11 of RAMPS 1.4 were used. The extruder's temperature control algorithm was developed in the Arduino C++ abstraction layer (Arduino.cc) and PlatformIO (PlatformIO Labs, Minks, Belarus). This program was designed using the Arduino PID Library (https://www.arduino.cc/reference/en/libraries/pid/). Software requirements included:

- Firmware: Marlin firmware on Arduino Mega, which contains the RAMPS v1.4.
- Slicer: Ultimaker Cura.
- Interface: Pronterface (https://www.pronterface.com/).
- Thermal Control Software: code editor compatible with C++. In this case, Visual Studio Code (VSC, Microsoft Corporation, Redmond, WA, U.S.) was used, in which the PlatformIO was installed. This algorithm is available from the corresponding authors on request.

In **Figure S3**, the marlin lines that need to be modified for the printer's and the extruder's normal functioning can be seen. Note that the firmware indicates that the printer has two extruders.

2.2 Experimental Methods

2.2.1 Formulation and printing of a thermo-curable ink based on κ-carrageenan (κ-c)

Kappa-carrageenan (κ-c) was purchased from Sigma-Aldrich (St. Louis, MI, U.S.). The protocol to formulate this ink can be found elsewhere [31]. Briefly, for the formulations without cells, a 15 mg mL^{-1} κ-c (15κ-c) solution was prepared in MilliQ water (Millipore, Merck, Darmstadt, Germany) under continuous stirring on a hotplate at 80º C until fully dissolved. This solution was then kept at 37º C prior to printing and food colouring was added to facilitate the visualisation of the printed materials. This was then transferred to a 3 mL printing cartridge (Nordson EFD Optimum) with a piston (Nordson EFD Optimum). Unless otherwise stated, a 0.33 mm diameter (23-Gauge) blunt needle was used (Nordson EFD Optimum). The printing temperature was set at 22º C, and the printing speed was set to 15 mm s^{-1} with a layer height corresponding to the inner diameter value of the tip used, i.e., 0.33 mm. Finally, the 15κ-c ink flow rate was set to 4% in PronterFace.

2.2.2 Printability Assessment

The assessment of the printability (Pr) was based on previous works [32] using Equation 1:

$$Pr = \frac{L^2}{16A} \qquad (1)$$

where L (mm) is the perimeter and A (mm^2) is the area of one pore.

Printability was evaluated by printing three 15 × 15 mm meshes containing nine pores, and two layers height (0.5 mm), with a printing speed of 15 mm s^{-1}. A 25-Gauge (inner diameter of 0.25 mm) blunt precision tip (Nordson EFD Optimum) was used to fabricate these structures. Three models (N=3) were printed using a G-code file created by the authors to print four lines in the Y direction and four in

the X direction, creating the nine pores mesh. After printing, optical microscopy images of the meshes were taken and the perimeter and area of interconnected channels was obtained using ImageJ software (ImageJ 1.51f, National Institutes of Health, Bethesda, MD, USA) (n=5) to calculate Pr.

2.2.3 Assessment of Prototype Calibration and Acceptance

A series of experiments were conducted to assess the functionality of the 3D bioprinter. Initially, water was used to test the deposition mechanism, and once its operation was confirmed, the three axes, including the offset of the printing plate, were calibrated. Five calibration models were used to assess the prototype's resolution, using either one or both extruders simultaneously, as detailed below. 3D models were generated on SolidWorks and exported as STL files (available under request). Printing trajectories were created by Ultimaker Cura and G-code files were modified using specially written scripts to adapt them to the properties of the printhead.

- **Parallelism assessment:** This test was performed following ISO 230-1:2012. Four 40 mm lines, spaced by 5 mm, were printed in this test with only one layer in the X direction and four in the Y direction to check the parallelism in these two axes, using both extruders (N=3, n=3, i.e., three different prints, with three measurements per print). After printing the models, the distance between lines was evaluated using ImageJ software and the angular error calculated using Equation 2.

$$\tan\theta = \frac{X_1 - X_2}{L} \qquad (2)$$

- **Lines for perpendicularity:** Two 40 mm long lines were printed in this test with only one layer, one in the X direction and the other in the Y direction, to evaluate the angle formed at their intersection. This test was performed using only one extruder, but the same strategy was applied using both extruders, with extruder 1 printing along the X direction and extruder 2 in Y (for each condition, N=3, n=2). According to ISO 230-1:2012, when the perpendicularity error is permitted in only one direction, that direction must be identified (greater or less than 90°).

- **Precision assessment:** The precision test was carried out according to ISO 230-2:2014. The bioprinter was programmed to move the extruder along an axis by depositing ink on several collinear lines and then moving along the other axis, depositing lines again, printing crosses with 15 mm long and then measured to check if they met the target positions. The speed of the extruder was constant throughout the test period. The different distances between the crosses in the X and Y directions (L= 25 mm) and the respective deviation from the right spot (ΔL) were measured. This test was performed for both extruders separately and simultaneously (for each extruder and each direction, N=2, n=3).

- **Printing of concentric squares:** A previously reported protocol was followed to perform this test [33]. Four concentric empty squares, with sides of 8, 12, 16, and 20 mm, respectively, were independently printed with one layer by each extruder. Each square was lined up with the other squares in X-Y directions. Separate measurements were taken for the X-Y sides of each square. The difference between the dimensions of the extruded model and the values of the CAD model were used to estimate the dimensional errors for this model. Three models were printed by each extruder, and for each square two measures were taken (N=3, n=2).

- **Printing of concentric circles:** This assay was performed following previous works [34]. Four concentric empty circles, with different diameters 8, 12, 16 and 20 mm and with one layer, were printed. XY-axes movements are simultaneously included in circles. Each circle's diameter was measured and compared to its theoretical value to determine the accuracy of the XY-axes' combined movement, as previously detailed (N=3, n=2).

For all the previous assessments, the individual evaluation of the parameters was performed through ImageJ software.

2.2.4 Formulation and printing of a bioink

L929 mouse fibroblasts were used for the formulation of the bioink. These were cultured in Dulbecco's Modified Eagle's Medium (DMEM, Thermo Fischer Scientific, Waltham, MA, U.S.) with 10% Fetal Bovine Serum (FBS, Thermo Fischer) and 1% penicillin/streptomycin (Sigma-Aldrich). Media was changed every two to three days. Cells were incubated at 37 °C in a 5% CO_2 atmosphere and passaged when 80% confluent using a trypsin/EDTA solution (Sigma-Aldrich).

To formulate the bioinks, a 9 mg mL^{-1} κ-c solution (9κ-c) was prepared in a proprietary media following previous works [31] and sterilised at 121 ºC, during 20 min, in an autoclave. After sterilisation, the cells, at a concentration of 1 000 000 cells mL^{-1}, were incorporated to this bioink and loaded into the printing cartridge, as previously mentioned.

The three rings (n=3) presented an inner diameter of 13.28 mm and a wall thickness twice the diameter of the tip, i.e, 0.66 mm. Contrary to the other models presented in this work, the rings were printed inside a laminar flow cabinet to ensure sterility, with a bioink flow rate of 3%, imposed in Pronterface at 37ºC. Once the bioprinting process was concluded, culture medium was added, covering the structures, supplemented with KCl to reach a final concentration of 0.05 M. This medium was changed at day every 3 days for 7 days.

2.2.5 Cell Viability Characterization

A live/dead assay was used to assess the cell viability in the bioprinted constructs. 1 µM calcium AM (Sigma-Aldrich) in phosphate-buffered saline (PBS, Thermo Fischer Scientific) was used to stain live cells and a solution of 4 µM ethidium homodimer I (Sigma-Aldrich) in PBS was used to stain dead cells. Stained cells were incubated for 30 minutes protected from direct light. Images were then taken on a Leica DMI3000B fluorescence microscope (Leica Microsystems, Wetzlar, Germany). Three independent samples were used to quantify the number of live and dead cells per image, where three images per scaffold were used in this calculation, using ImageJ software (N=3, n=3).

2.2.6 Formulation and printing of a photocurable ink

The GelMA synthesis was carried out following a previously reported protocol [35]. Briefly, gelatine powder from porcine skin (Sigma-Aldrich) was dissolved in Dulbecco's phosphate-buffered saline (DPBS, Thermo Fischer Scientific) at 50ºC at a concentration of 100 mg mL^{-1} and stirred until fully dissolved. Methacrylic anhydride (Sigma-Aldrich) was then added dropwise until reaching a final concentration of 8% (v/v). This solution was left stirring for 3 h at 50ºC. Once this step was completed, DPBS was added to reach a final gelatine concentration of 20 mg mL^{-1}. Then, the solution was placed in a dialysis tubes (Sigma-Aldrich) of 2 000 molecular weight cut-of (MWCO), in ultrapure water at 50 ºC for four days. Water was changed twice daily. After the dialysis, the solution was placed at -80 ºC for 24 h, lyophilized for four days and stored at -80 ºC wrapped in aluminium foil until further use.

Lyophilized GelMA was reconstituted at a final concentration of 5% (wt/v) in DPBS at 50 ºC in a jar shielded from light. 0.5% (wt/v) lithium phenyl-2,4,6-trimethylbenzoylphosphinate (LAP, Sigma-Aldrich) was added to this solution and left stirring at 50 ºC for three hours prior to printing.

This solution was then transferred to an amber-coloured 3 mL printing cartridge (Nordson EFD Optimum) with a piston and a 0.61 mm (20-Gauge) blunt needle. Printing parameters consisted of a printing speed of 15 mm s^{-1}, an ink flow rate of 10 % imposed through the Pronterface software and a temperature of 38 ºC. The UV curing involved exposing the printed geometry to UV radiation emitted by the LED at the bottom of the extruder. The extruder repeated the printing path at the end of the process, with half of the printing speed, i.e. 7.5 mm s^{-1}, at a distance of 0.5 mm height from the obtained geometry. Structures printed consisted of small discs, with a diameter of 10 mm and with only one layer, i.e., 0.61 mm high.

2.2.7 Statistical Analysis

Results were reported as mean ± standard deviation (SD). GraphPad Prism v9.4.1 (GraphPad, San Diago, CA, USA) was used to conduct t-student tests for statistical significance.

2.3 Prototype setup & Software programming

2.3.1 Printhead Assembly and Control Box

As shown in **Figure 3a**, the extruder assembly began by fixing the aluminium block on the sides of the extruder drawer with four M3 screws. Both the Peltier module and the heat sink are glued with thermal paste (AG TERMOPASTY, Soloky, Poland) and therefore fixed to the aluminium block. Four M3 screws supported the fan, placed in the opposite side of the aluminium block, and the cover was closed with four M2 screws. The shell was inserted into the extruder support and, in turn, guided through the rails system. Two pins were inserted to prevent the cartridge from opening during the printing job and fixing it in the correct position. Finally, the shell cover contained air outlets and was fixed to the shell through two M2 screws. After the two extruder drawers were assembled, the cables for the thermistor, Peltier module, UV LED, and fan must were arranged to exit from the side of the shell and pass through the lateral grooves that were designed to contain and guide them. As seen in **Figure 3b**, the captive axis was attached to the top of each of the non-captive stepper motors using 50 mm long M3 screws. These screws replaced the original screws that close the motors. The motors were inserted into the printhead support and then screwed using four M3 screws, 7.5 mm long. The electronics box worked as a printer driver since the connections that powered the various electrical devices exit from this critical component. The box had two outputs and switches that were used to separate the cables for the temperature control unit and UV curing from the cables for the deposition motion control. **Figure 3c** shows that this box presented two 12 V power supplies that independently powered the motion and the temperature control. The power control circuit incorporated two BTS7960 modules, two LCDs, four fans, two breadboards, and two Arduino Mega 2560 boards. One LCD was connected to the Arduino Mega 2560, which controlled movement and included a menu that enabled control to all the printer's axis, auto-home, and incorporated a secure digital card (SDC) reader. The temperature of each extruder was displayed on the second LCD. Finally, this driver had two USB ports for connecting to Arduinos. A complete image of the assembled bioprinter can be seen in **Figure 3d**.

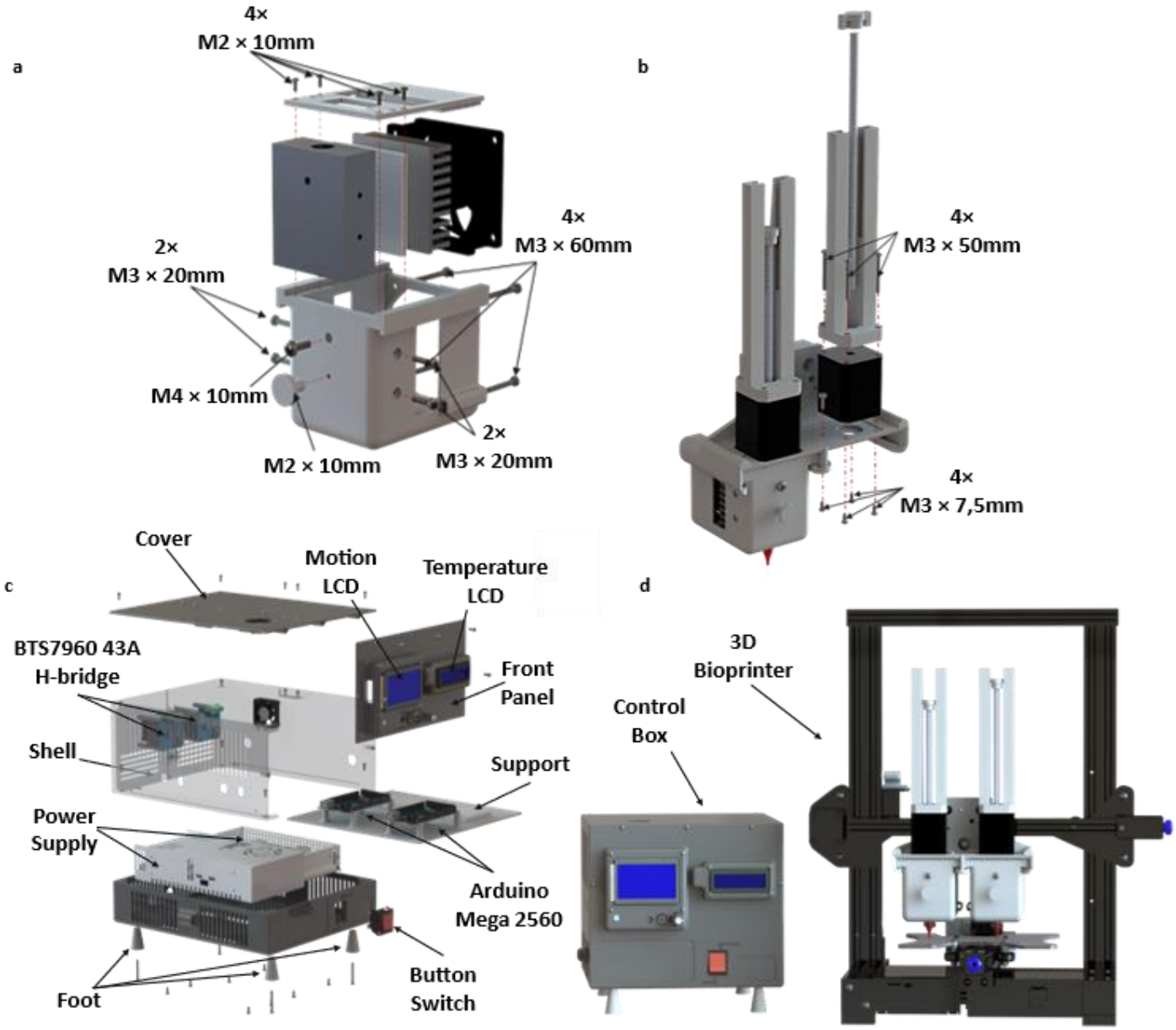

Figure 3. Design of the 3D extrusion bioprinter: **(a)** Bioprinter's extruder drawer CAD model view. **(b)** Syringe pump extrusion system CAD model view. As can be seen the extruder's support contains M3 holes to fix the two stepper motors and rails through which the shell rails are guided. **(c)** Equipment control box CAD model view. The electronic box is responsible for feeding and controlling all the physical systems of the printer and includes the circuit that regulates the power of the Peltier modules shown in **Figure S4.** On the other hand, as seen in the image on the left, the support contains chamfers precisely in the air outlet of the drawer cover. **(d)** Cad design of the prototype apparatus: the first 3D extrusion bioprinter with temperature control and UV curing, designed and fabricated at Instituto Superior Técnico, Lisbon, Portugal

2.3.2 Prototype Main Specifications

The general specifications of the prototype can be seen in **Table 2**.

Table 2. 3D bioprinter main specifications. The specifications in italics are the ones that remain similar to the FDM-type Creality Ender-3 V2 3D printer used as chassis. *****The dimensions of the syringe barrels compatible with the prototype can be found on Nordson's website (length: 73 mm; diameter: 11.1 mm).

Extruders	2 Cores
Photocuring	LED-365 nm
Printing Technology	FDM
Build Volume	*220×220×150 mm*
Compatible Syringes	3 mL plastic/metal*
Minimum Temperature	2 ºC
Maximum Temperature	50 ºC
Maximum Force Output	320 N
Construction	Aluminium, PETG
X, Y Precision	0.006 mm
Z Precision	0.001 mm
Dimensions	*475×470×620mm*
Weight	7 kg

2.3.3 Setting up Ultimaker Cura and G-Code Modifications

Instructions to set the Ultimaker Cura software (Ultimaker Cura v5.0, Ultimaker B.V., Utrecht, Nederland) can be seen in the supporting information. The G-Code file generated by the Cura software only contained the commands for moving the extruder along the three axes and instructions for depositing the ink along the path. These commands do not consider the positioning of the printing substrate in the printing stage. Therefore, a collision may occur between the syringe tip placed in the extruder drawer and the substrate. On the other hand, it was not possible to generate commands to control the UV curing functionality through the slicing program. Therefore, changes must be made according to the various specifics of the object to be printed and the printing substrate. Further instructions on how to set the commands for printing with one or two extruders and UV light can be seen in the supporting information.

2.3.4 Printing Routine

The machine's operating routine is similar to a conventional FDM printer. However, the temperature control system of the two extruders is independent of the motion control and, therefore, must be controlled separately. The procedure for operating the 3D extrusion Bioprinter can be seen in the Supporting Information.

3 Results and Discussion

3.1 Ink's printability & print resolution accuracy

The printability of the 15κ-c ink was assessed by printing a one-layered mesh. All the measured samples presented a mean printability value of 0.995 (Figure 4a). This lies within the acceptance region as the mean is closer to the ideal value (Pr = 1), showing higher values than similar works found in the literature [36, 37]. In this work, the authors used a three-axis dispensing robot Fisnar 4200N.2 to print the same material at room temperature, obtaining a mean printability value of 0.91. Considering these results, we can confirm that the prototype developed in this work potentially offers better printability values, comparing to the ones obtained using a commercial bioprinter, for the same inks, due to a lower printing speed and greater control over the deposition rate, features obtained through the integration of a screw-driven deposition system and the syringe's temperature control system.

The parallelism assessment was initially performed only with extruder 1 (E1) in both directions, to evaluate whether the X-axis or the Y-axis were warped. As shown in **Figure 4b**, the results obtained for E1 demonstrate the high accuracy of the whole printhead, since the results obtained are all close to the obtained mean. The mean values consisted of 0.0019º for E1, and 0.0044º for E1+E2 in the X direction, being close to the ideal result (θ = 0º). These results allow us to conclude that the printhead, as a whole, also presents high accuracy. Regarding the results obtained using the two extruders simultaneously, i.e., E1 and extruder 2 E2, the mean value obtained was 0.0024º for the Y direction, which is closer to the ideal value (θ = 0º) than the mean value obtained for the X direction. This difference in results could be due to the introduction of an erroneous offset value between the two extruders. The theoretical X-distance between the two syringe tips is 82 mm. However, since the parts were obtained by 3D printing and therefore present slight distortions related to the nature of the manufacturing process, this value, in reality, is slightly lower. That is why the two central lines presented in **Figure 4b** are closer than the outer ones. There was also some error in the Y direction, where the green lines are slightly off-side. The offsets in X and Y were changed to eliminate the presented errors. Naturally, the offset value varies from prototype to prototype since the elements are 3D printed and different distortions may appear. Thus, it is recommended by the authors that the users, after the assembly of the prototype, perform this acceptance test to determine the theoretical offset values.

Likewise, the accuracy and precision of E1 and E2 in a perpendicularity test can be similar since the movement of these two extruders depend on the same axis system. In

the first test, we evaluated the perpendicularity of the X and Y axis through E1, resulting in a mean of 89.866º (**Figure 4c**). This demonstrated that the results obtained presented high accuracy, since the error distribution is uniform along all readings and the mean and ideal values are very close (θ = 90º). It was also possible to observe that E1 was more accurate than E2, as the mean of E2 is 0.4º above the expected value 90º. However, there are no statistical differences between the results obtained for these two extruders when they are set to print independently. However, E1 and E2 are coupled to the same printhead, therefore, the movement in the XY and Z planes will always be the same, which is why the results are similar.

The offset adjustment proposed in the previous point had yet to be implemented to impose a real X and Y distance between the two extruders. Therefore, this offset deviation was present in this test, but it did not interfere with the type of error here evaluated. The data obtained using the two extruders simultaneously present results similar to the ones obtained by E2 (mean: 89.5993º) since the distribution is identical. However, a significant difference was observed between E2 and E1+E2. In practice, this difference is not critical, as for both extruders, the mean and ideal values are again close of each other and their differences could be explained due to inaccuracies of the measurements taken by ImageJ.

For the precision assay, the results obtained for E1 and E2 are statically different since their means and standard deviation do not overlap, consisting on 24.67 ± 0.2276 mm, and 25.03 ± 0.1746 mm, respectively (**Figure 4d**). However, as it can be seen, the variations registered do not exceed one millimetre, and in many measurements, the values were within the -0.5 to 0.5º range. Although there is a difference between E1 and E2, we can state that both means are close to the theoretical value (L = 25 mm), with E2 being closer to this value. One possible explanation for such differences could be the different deposition rates. Despite an effort to obtain identical filaments in both prints, when testing only E1, it was noted that the deposition rate was unnecessarily high. Therefore, the

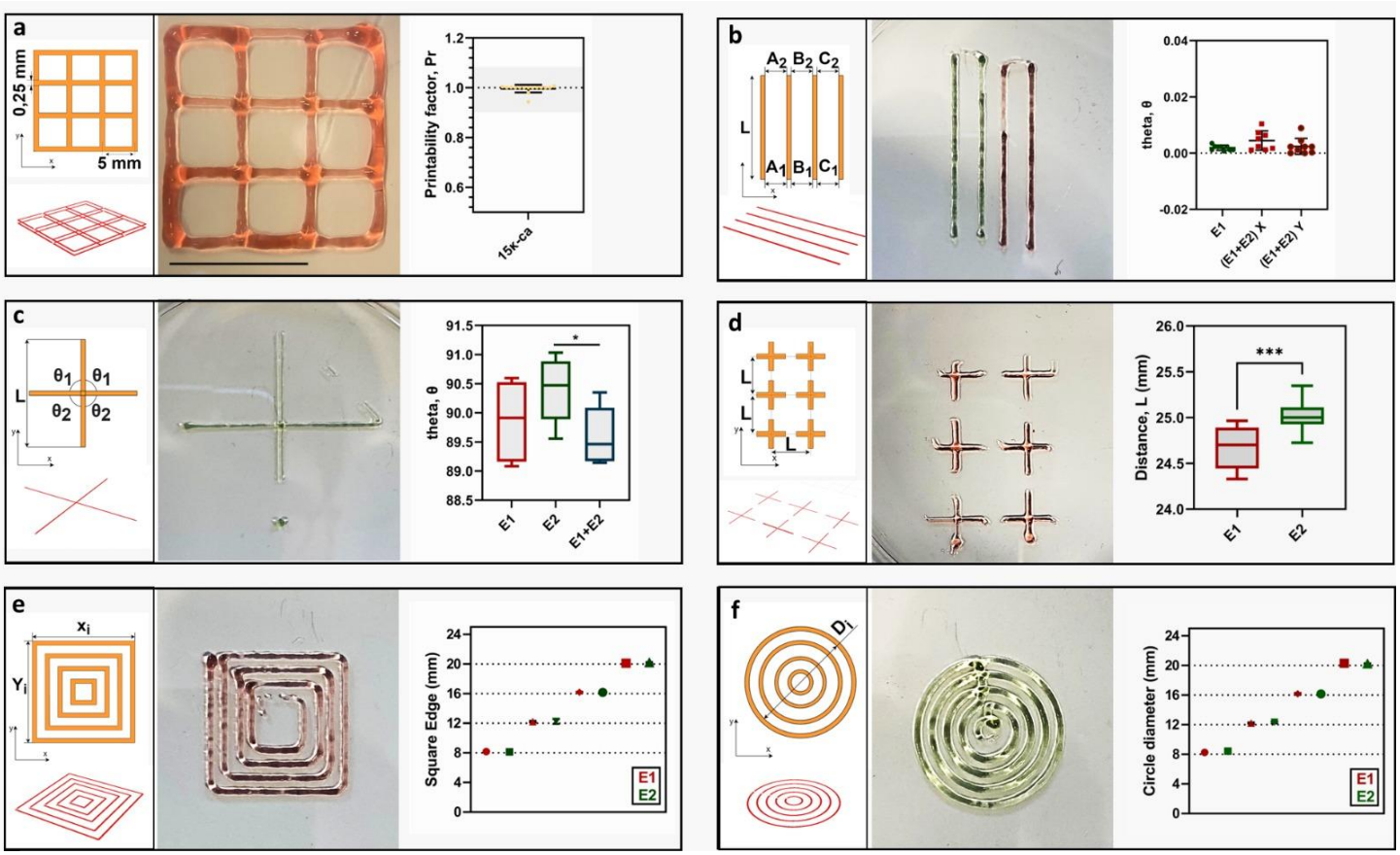

Figure 4. Schematic and optical representation of the 3D calibration models (a) 15κ-c ink's printability factor with individual factor values. According to [32], the grey area denotes the range of acceptable ink printability (from 0.9 to 1.1). Scale bar 10 mm. (b) Parallelism tests models and individual results. The parallelism between the two extruders in both directions was evaluated by printing two lines with E1 (red ones) and another two with E2 (green ones). (c) Perpendicularity test models and results (p* =0.0242). (d) Precision tests compound by several points distributed in the X and Y axis, separated by 25 mm (p***=0.0003). (e) Concentric Squares aligned with XY-axis and its respective dimensional error. (f) Concentric circles aligned with XY-axis and its respective dimensional error

filaments obtained were thicker, resulting in a greater dispersion of the measurements.

To finalize the accuracy assessment two different types of concentric structures were printed. Firstly, concentric squares were printed using the two extruders independently. These models allowed us to confirmed if the offset deviations previously detected by the parallelism and perpendicularity studies were constant and whether they could be corrected when constructing larger geometries. In this case, each edge is printed, moving only one of these axes independently. Therefore, by measuring the edges of each square, we can confirm if they remain concentric and evaluate whether there is any dimensional error specific to the X or the Y axes. As can be seen in **Figure 4e**, there is no difference between the dimensional errors in E1 and E2. On the other hand, all the results are close to the theoretical values 8, 12, 16, 20 mm. It is important to note though, that when printing geometries with 90º corners with these hydrogels, it is difficult to get a perfect vertex. Secondly, printing four concentric circles with one layer was used as a different calibration model. Circular, cylindrical, and semi-spherical models can be employed to assess the printing resolution of the printhead, while both XY axes are moving simultaneously, and each extruder is operating independently. As seen in **Figure 4f**, there is a deviation from the theoretical results for smaller diameters (8 to 12 mm). This means that the larger the internal diameter, the smaller the dimensional error. This could be due to small vibrations taking place when the X and Y axes move simultaneously.

3.2 Assessment of Cell Viability and Proliferation

A 9k-c bioink was used to assess cell viability and proliferation and printing parameters optimised. After the incorporation of the L929 cells, the different printing conditions were used without observing differences in the formation of the printing filament.

The bioprinted three rings (N=3), whose dimensions are specified in section 2.2.4 (**Figure 5a**) were preserved in culture medium at 37ºC for seven days. As shown in **Figure 5b**, the cells were able to populate the bioprinted structure and, although most of them still presented a round shape, some of the cells started to elongate. A live/dead fluorescence assay confirmed the high viability values after bioprinting (**Figure 5c** and **Figure 5d**), presenting mean values of 96.5833% for N1, 96.2567 for N2 and finally 96.4733 for N3. These values are within the parameters reported by prior investigations on extrusion-based bioprinting [8], namely when comparing the results obtained by Sanz-Garcia et al., which developed a 3D bioprinter that also presents temperature control [29].

On the other hand, when comparing the cellular viability results obtained with those previously published by Marques et al. [37] for bioprinting the same cells on the same bioink using a different printer, we observed in our study a slightly higher values of cell viability. We hypothesise that this could be due to the following: (i) Our structures were printed at an approximate printing rate of about 15 mm s^{-1}, in contrast to the printing rate of 20 mm s^{-1} used in the previous work, which can lead to a higher shear-stress, affecting cell viability. (ii) This prototype incorporates temperature control on the printing cartridge, keeping the temperature constant during printing, which promotes a stabilization on material's mechanical properties, namely viscosity, avoiding the need to adjust the imposed forces to guarantee the extrusion of the bioink, thus imposing less shear stress.

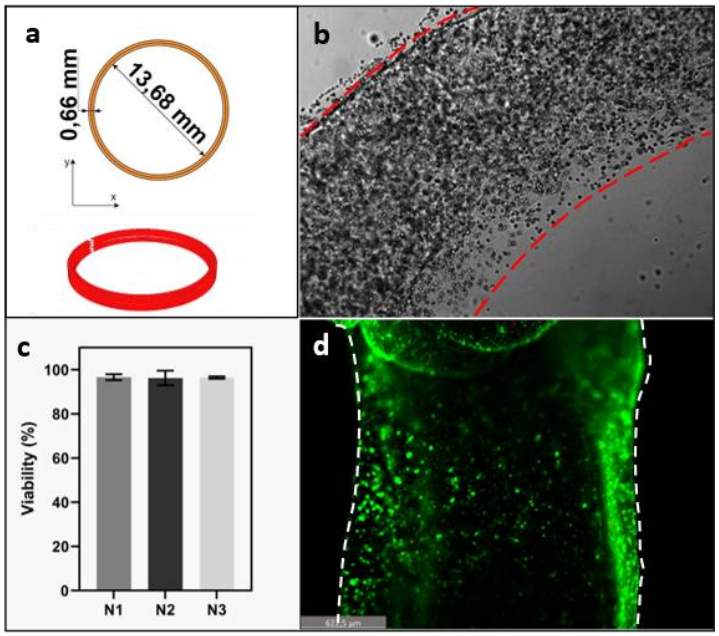

Figure 5. Analysis of cell viability in the 3D bioprinted constructions. (a) Schematic model of the ring printed on the assay to determine cell viability consisting on a 13.68 mm in diameter ring with a wall thickness of 0.66 mm and is five layers in height. (b) Brightfield image of mouse L929 fibroblasts that were bioprinted using 9k-c bioink, with dotted red lines showing the edges of the structure after 3 days of culture. (c) Cell viability of the three rings printed using the 23G blunt tip after 7 days of culture obtained through the fluorescence images (d) after the Live/Dead staining (N=3, n=3).

3.3 UV Curing

Printing parameters with GelMA were optimised until a linear structure was obtained with a cross-section that corresponds to the internal diameter of the blunt needle, which has a diameter of 0.61 mm. This set of tests showed that this ink was very thermosensitive since the needle clogged several times between prints. As mentioned in section **2.1.4**, to perform UV curing, we decided that the

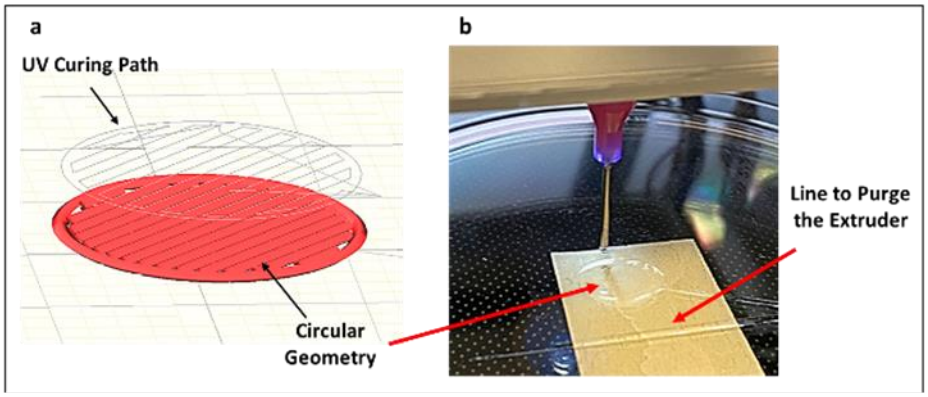

Figure 6. Photocrosslinking of GelMA by exposing it to UV radiation. (a) Pronterface scheme of the circular geometry printed to test the UV crosslinking capabilities of the 3D bioprinter. The red lines correspond to the printed disk exposed in (b), and the grey lines correspond to the path that the UV LED took to cure the GelMA-based hydrogel. (b) Image of circular geometry being printed.

most effective way to print this material was to use the G-Code commands of the printed geometry to also control the LED, as the path shown in grey lines (**Figure 6a**). Therefore, after each ink layer deposition, the instructions for ink deposition were repeated, but with the extruder inactivated, and the LED was turned On. These process of alternating ink deposition and UV cured was repeated, but with the Z-coordinate incremented to obtain several stack layers.

The protocol for using the UV LED on each of the extruders is presented in the supporting information. In order to build a perfect circular disc-shaped geometry, i.e., without lack of material, it was decided to print a 40 mm long line before starting the construction of the disc to purge the extruder and thus unclog the syringe blunt tip, as can be seen in **Figure 6b**. In the supporting information, we present two videos of GelMA printing, in which we can compare the disks' morphology with and without UV radiation exposure (**Video S1**, **Video S2**). As seen in **Video S2**, the polymer crosslinks after UV exposure, and it is possible to manipulate the disc with a small spatula keeping its shape and consistency.

4 Conclusions

The main conclusions taken from this work are summarised below:

- An open-source 3D extrusion bioprinter was designed in this work, based on an Ender 3-v2 motion system. Due to the incorporation of temperature control and UV light on the printing heads, this prototype is compatible with thermo- and photocurable materials. Additionally, the presence of two independent extruders allows to print with two different materials, demonstrating the high versatility of this prototype.
- The maximum extrusion force of the bioprinter is 320 N. With a modular architecture that enables 3 mL syringes, our printhead could be a low-cost alternative to commercial bioprinters. The printing temperature can be carefully adjusted from 2 to 50 ºC, similar to other commercial [16] and non-commercial [29], enabling printing with various bioinks of different viscosities. The fact that the suggested design can be easily modified and installed in the vast majority of affordable open-source 3D printers gives it an edge over competing systems.
- The printing resolution assessed by the dimensional tests, including the printability test, shows that although the positional precision of the 3D printers employed is lower than other expensive machines on the market, it may still be sufficient for working on various TE applications. This prototype could also be employed in bioprinting achieving cell viabilities above 97%.
- The manufacturing of the printhead and electronic box relied nearly entirely on 3D FDM printing, which is a low-cost method, demonstrating the value of additive manufacturing methods and their potential in various engineering fields.

Thanks to its characteristics, portability, and user-friendliness, the equipment may be quickly applied in TE research, specifically in 3D bioprinting low-budgeted groups, since the total cost of goods was less than 1000 EUR. Due to the high cost of the currently available commercial options, the by-products produced by 3D bioprinting are often expensive. Therefore, this prototype has the potential to promote the development of novel 3D bioprinting strategies and materials with a great price-quality ratio.

5 References

[1] 'Organ Donation and Transplantation', Human Rights Channel. https://human-rights-channel.coe.int/organ-donation-en.html (accessed Feb. 08, 2022).

[2] C. J. E. Watson and J. H. Dark, 'Organ transplantation: historical perspective and current practice', Br J Anaesth, vol. 108 Suppl 1, pp. i29-42, Jan. 2012, doi: 10.1093/bja/aer384.

[3] K. V. Wong and A. Hernandez, 'A Review of Additive Manufacturing', ISRN Mechanical Engineering, vol. 2012, pp. 1–10, Aug. 2012, doi: 10.5402/2012/208760.

[4] I. T. Ozbolat and M. Hospodiuk, 'Current advances and future perspectives in extrusion-based bioprinting', Biomaterials, vol. 76, pp. 321–343, Jan. 2016, doi: 10.1016/j.biomaterials.2015.10.076.

[5] A. Dick, B. Bhandari, and S. Prakash, '3D printing of meat', Meat Science, vol. 153, pp. 35–44, Jul. 2019, doi: 10.1016/j.meatsci.2019.03.005.

[6] G. Potter et al., 'A More Open Approach Is Needed to Develop Cell-Based Fish Technology: It Starts with Zebrafish', One Earth, vol. 3, no. 1, pp. 54–64, Jul. 2020, doi: 10.1016/j.oneear.2020.06.005.

[7] F. Pati, J. Jang, and J.-W. Lee, 'Extrusion Bioprinting', 2015, pp. 123–152. doi: 10.1016/B978-0-12-800972-7.00007-4.

[8] S. V. Murphy and A. Atala, '3D bioprinting of tissues and organs', Nature Biotechnology, vol. 32, no. 8, Art. no. 8, Aug. 2014, doi: 10.1038/nbt.2958.

[9] T. Hinton et al., 'Three-dimensional printing of complex biological structures by freeform reversible embedding of suspended hydrogels', Science Advances, vol. 1, pp. e1500758–e1500758, Oct. 2015, doi: 10.1126/sciadv.1500758.

[10] D. J. Shiwarski, A. R. Hudson, J. W. Tashman, and A. W. Feinberg, 'Emergence of FRESH 3D printing as a platform for advanced tissue biofabrication', APL Bioengineering, vol. 5, no. 1, p. 010904, Mar. 2021, doi: 10.1063/5.0032777.

[11] N. Hong, G.-H. Yang, J. Lee, and G. Kim, '3D bioprinting and its in vivo applications', Journal of Biomedical Materials Research Part B: Applied Biomaterials, vol. 106, no. 1, pp. 444–459, 2018, doi: 10.1002/jbm.b.33826.

[12] J. S. Miller et al., 'Rapid casting of patterned vascular networks for perfusable engineered three-dimensional tissues', Nature Mater, vol. 11, no. 9, Art. no. 9, Sep. 2012, doi: 10.1038/nmat3357.

[13] B. Duan, L. A. Hockaday, K. H. Kang, and J. T. Butcher, '3D Bioprinting of heterogeneous aortic valve conduits with alginate/gelatin hydrogels', Journal of Biomedical Materials Research Part A, vol. 101A, no. 5, pp. 1255–1264, 2013, doi: 10.1002/jbm.a.34420.

[14] F. Guillemot, V. Mironov, and M. Nakamura, 'Bioprinting is coming of age: Report from the International Conference on Bioprinting and Biofabrication in Bordeaux (3B'09)', Biofabrication, vol. 2, no. 1, p. 010201, Mar. 2010, doi: 10.1088/1758-5082/2/1/010201.

[15] S. M. Ehsan, K. M. Welch-Reardon, M. L. Waterman, C. C. W. Hughes, and S. C. George, 'A three-dimensional in vitro model of tumor cell intravasation', Integr Biol (Camb), vol. 6, no. 6, pp. 603–610, Jun. 2014, doi: 10.1039/c3ib40170g.

[16] A. Tong et al., 'Review of Low-Cost 3D Bioprinters: State of the Market and Observed Future Trends', SLAS TECHNOLOGY: Translating Life Sciences Innovation, vol. 26, no. 4, pp. 333–366, Aug. 2021, doi: 10.1177/24726303211020297.

[17] A. Sanz-Garcia, E. Sodupe-Ortega, A. Pernía-Espinoza, T. Shimizu, and C. Escobedo-Lucea, 'A Versatile Open-Source Printhead for Low-Cost 3D Microextrusion-Based Bioprinting', Polymers, vol. 12, no. 10, Art. no. 10, Oct. 2020, doi: 10.3390/polym12102346.

[18] A. Krige, J. Haluška, U. Rova, and P. Christakopoulos, 'Design and implementation of a low cost bio-printer modification, allowing for switching between plastic and gel extrusion', HardwareX, vol. 9, p. e00186, Apr. 2021, doi: 10.1016/j.ohx.2021.e00186.

[19] Z. Gu, J. Fu, H. Lin, and Y. He, 'Development of 3D bioprinting: From printing methods to biomedical applications', Asian Journal of Pharmaceutical Sciences, vol. 15, no. 5, pp. 529–557, Sep. 2020, doi: 10.1016/j.ajps.2019.11.003.

[20] J. Y. Kim, E. K. Park, S.-Y. Kim, J.-W. Shin, and D.-W. Cho, 'Fabrication of a SFF-based three-dimensional scaffold using a precision deposition system in tissue engineering', J. Micromech. Microeng., vol. 18, no. 5, p. 055027, Apr. 2008, doi: 10.1088/0960-1317/18/5/055027.

[21] J. A. Reid, P. A. Mollica, G. D. Johnson, R. C. Ogle, R. D. Bruno, and P. C. Sachs, 'Accessible bioprinting: adaptation of a low-cost 3D-printer for precise cell placement and stem cell differentiation', Biofabrication, vol. 8, no. 2, p. 025017, Jun. 2016, doi: 10.1088/1758-5090/8/2/025017.

[22] J. W. Tashman, D. J. Shiwarski, and A. W. Feinberg, 'A high performance open-source syringe extruder optimized for extrusion and retraction during FRESH 3D bioprinting', HardwareX, vol. 9, p. e00170, Apr. 2021, doi: 10.1016/j.ohx.2020.e00170.

[23] A. Engberg, C. Stelzl, O. Eriksson, P. O'Callaghan, and J. Kreuger, 'An open source extrusion bioprinter based on the E3D motion system and tool changer to enable FRESH and multimaterial bioprinting', Sci Rep, vol. 11, no. 1, Art. no. 1, Nov. 2021, doi: 10.1038/s41598-021-00931-1.

[24] I. T. Ozbolat, H. Chen, and Y. Yu, 'Development of "Multi-arm Bioprinter" for hybrid biofabrication of tissue engineering constructs', Robotics and Computer-Integrated Manufacturing, vol. 30, no. 3, pp. 295–304, Jun. 2014, doi: 10.1016/j.rcim.2013.10.005.

[25] K. Pusch, T. J. Hinton, and A. W. Feinberg, 'Large volume syringe pump extruder for desktop 3D printers', HardwareX, vol. 3, pp. 49–61, Apr. 2018, doi: 10.1016/j.ohx.2018.02.001.

[26] N. Bessler et al., 'Nydus One Syringe Extruder (NOSE): A Prusa i3 3D printer conversion for bioprinting applications utilizing the FRESH-method', HardwareX, vol. 6, p. e00069, Oct. 2019, doi: 10.1016/j.ohx.2019.e00069.

[27] M. Milazzo et al., 'Additive Manufacturing Approaches for Hydroxyapatite-Reinforced Composites', Advanced Functional Materials, vol. 29, no. 35, p. 1903055, 2019, doi: 10.1002/adfm.201903055.

[28] K. Melanie et al., 'Ultra-Low-Cost 3D Bioprinting: Modification and Application of an Off-the-Shelf Desktop 3D-Printer for Biofabrication', Front Bioeng Biotechnol, vol. 7, p.184, Jul. 2019, doi: 10.3389/fbioe.2019.00184

[29] Sanz-Garcia Andres et al. 'A Versatile Open-Source Printhead for Low-Cost 3D Microextrusion-Based Bioprinting', Polymers, vol 12, p. 2346, Oct 2020, doi: 10.3390/polym12102346

[30] V. Klar, J. M. Pearce, P. Kärki, and P. Kuosmanen, 'Ystruder: Open source multifunction extruder with sensing and monitoring capabilities', HardwareX, vol. 6, p. e00080, Oct. 2019, doi: 10.1016/j.ohx.2019.e00080.

[31] D. M. C. Marques, J. C. Silva, A. P. Serro, J. M. S. Cabral, P. Sanjuan-Alberte, and F. C. Ferreira, '3D Bioprinting of Novel κ-Carrageenan Bioinks: An Algae-Derived Polysaccharide', Bioengineering, vol. 9, no. 3, Art. no. 3, Mar. 2022, doi: 10.3390/bioengineering9030109.

[32] L. Ouyang, R. Yao, Y. Zhao, and W. Sun, 'Effect of bioink properties on printability and cell viability for 3D bioplotting of embryonic stem cells', Biofabrication, vol. 8, no. 3, p. 035020, Sep. 2016, doi: 10.1088/1758-5090/8/3/035020.

[33] F. A. Cruz Sanchez, H. Boudaoud, L. Muller, and M. Camargo, 'Towards a standard experimental protocol for open source additive manufacturing', Virtual and Physical Prototyping, vol. 9, no. 3, pp. 151–167, Jul. 2014, doi: 10.1080/17452759.2014.919553.

[34] C. Polzin, S. Spath, and H. Seitz, 'Characterization and evaluation of a PMMA-based 3D printing process', Rapid Prototyping Journal, vol. 19, no. 1, pp. 37–43, Jan. 2013, doi: 10.1108/13552541311292718.

[35] P. Sanjuan-Alberte et al., 'Development of Conductive Gelatine-Methacrylate Inks for Two-Photon Polymerisation', Polymers (Basel), vol. 13, no. 7, p. 1038, Mar. 2021, doi: 10.3390/polym13071038

[36] Y. Chen, M.-L. Liao, and D. E. Dunstan, 'The rheology of K+-κ-carrageenan as a weak gel', Carbohydrate Polymers, vol. 50, no. 2, pp. 109–116, Nov. 2002, doi: 10.1016/S0144-8617(02)00009-7.

[37] S. Liu, W. L. Chan, and L. Li, 'Rheological Properties and Scaling Laws of κ-Carrageenan in Aqueous Solution', Macromolecules, vol. 48, no. 20, pp. 7649–7657, Oct. 2015, doi: 10.1021/acs.macromol.5b01922.

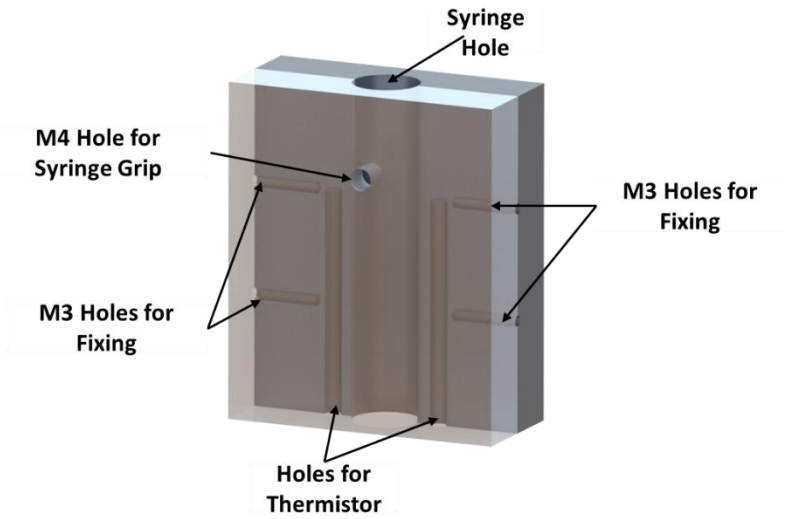

Figure S7. CAD model of syringe's aluminium heat sink. The block's geometric technical drawing can be found in the Annex, as it was machined to build the temperature control unit through machining processes carried out at LTO, Técnico, Lisbon.

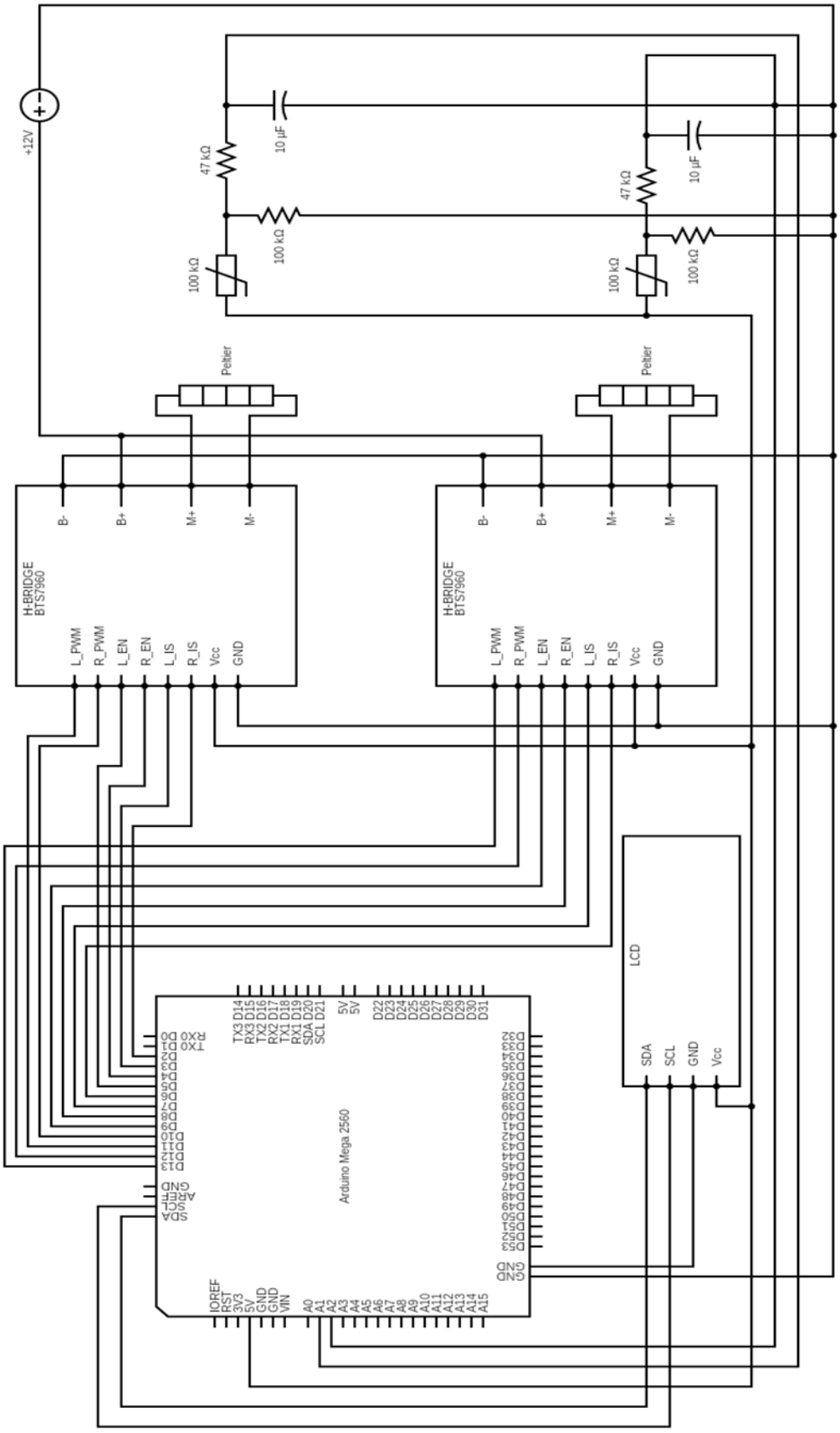

Figure S8. Circuit used in the prototype allows to regulate the Peltier modules supply voltage and invert their polarity to obtain a cooling or heating syringe temperature control.

```
118   #define BAUDRATE 250000
142   #define MOTHERBOARD BOARD_RAMPS_14_EEB
195   #define EXTRUDERS 2
199   #define DEFAULT_NOMINAL_FILAMENT_DIA 9.5
372   #define HOTEND_OFFSET_X  {0.0, 0.0}
512   #define TEMP_SENSOR_0 998
513   #define TEMP_SENSOR_1 998
885   #define X_DRIVER_TYPE DRV8825
886   #define Y_DRIVER_TYPE DRV8825
887   #define Z_DRIVER_TYPE DRV8825
896   #define E0_DRIVER_TYPE DRV8825
897   #define E1_DRIVER_TYPE DRV8825
949   #define DEFAULT_AXIS_STEPS_PER_UNIT{ 160, 160, 800, 3200}
1414  #define X_BED_SIZE 220
1415  #define Y_BED_SIZE 220
1423  #define Z_MAX_POS 150
```

Figure S9. Marlin modifications.

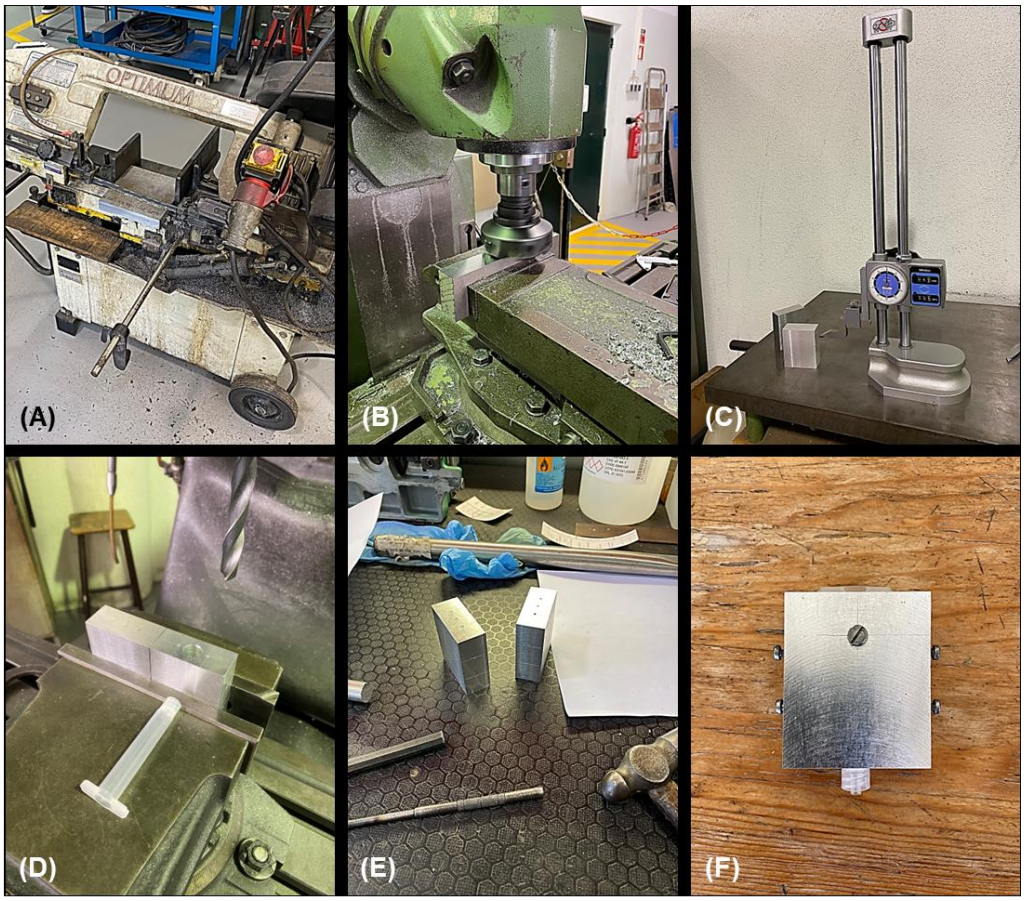

Figure S10. Machining techniques used to manufacture the two aluminium blocks present in the machine. The different phases are ordered chronologically and alphabetically: (A) Cutting: (B) Milling; (C) Point Mark with a height measurement gauge; (D) Drilling; (F) Threading; (G) Syringe's Aluminium Heat Sink with screws and a syringe inserted.

Table S3. Equipment components acquired from third parties.

Part	Amount	Cost per unit [€]	Total Cost [€]	Material/Type
Creality Ender-3 V2	1	324,39	324,39	3D printer
Peltier Thermoelectric Module 14.2V 57W	2	17,45	34,90	Module
Sunon Fan 60x60x25mm 12VDC 0,13A 1,56W	2	9,63	19,26	Fan
Aluminium Heat Sink 53,3x53,3x16,51mm	2	4,92	9,84	Heat Sink
UV LED 5mm, Wavelength: 365nm	2	1,11	2,22	UV LED
Motor Nema 17 Non-Captive 48mm	2	54,84	109,68	Stepper Motor
H-Bridge BTS7960 43A	2	18,29	39,58	Module
Arduino MEGA 2560	2	36,90	73,8	Module
RAMPS 1.4 Arduino MEGA Shield	1	11,07	11,07	Module
DRV8825 Stepper Motor Driver	5	3,90	19,5	Module
Thermistor 100k NTC	2	2,10	4,20	Thermistor
RAMPS 1.4 12864 LCD Module	1	24,60	24,60	LCD
16x2 I2C LCD Module	1	8,18	8,18	LCD
Power Supply 12V 25A 300W	1	17,25	17,25	Power Supply
Power Supply 12V 10A 120W	1	12,46	12,46	Power Supply
Rocker Switch	1	1,45	1,45	Switch
Fan 30x30x5mm 12V	2	4,15	8,30	Fan
Fan 40x40x5mm 12V	2	5,69	11,38	Fan
Capacitor 10uF	2	0,20	0,40	Capacitor
Breadboard	1	2,5	2,5	Breadboard
Resistors (various)	6	0,10	0,6	Resistor
Total	-	-	735,56	-

Table S4. Printing parameters used to print all the components that integrate the extruder-head structure, components, and shell.

Layer Height [mm]	0,2
Wall Thickness [mm]	0,8
Infill Density [%]	35,0
Infill Pattern	Cubic
Printing Temperature [ºC]	235,0
Build Plate Temperature [ºC]	70,0
Print Speed [mm/s]	50,0
Fan Speed [%]	25,0

Setting up Ultimaker CURA

After installing the Ultimaker Cura, open the software and click on 'Prepare' and select the 'Printers' tab and create a new custom 3D printer. Then select the new printer and then go to 'Machine Settings'. In the 'Printer' settings set the 'Build plate shape' to 'Rectangular' with 'X = 220 mm', 'Y = 220 mm' and 'Z = 150 mm'. Change the 'Number of Extruders' to 2, and the 'Gantry Height' to 150 mm. Then select the 'Extruder 1' and in this tab, change the 'Compatible material diameter' to 9.5 mm (which corresponds to the inner diameter of the used syringe barrel), 'Nozzle offset X' to -41,0 mm, 'Nozzle offset Y' to 0,0 mm and 'Colling Fan Number' to 0 and, finally the 'Nozzle Size' to the same value of the inner diameter of the used syringe tip. After changing the settings of the extruder 1, select the 'Extruder 2' tab and insert the same values of 'Extruder 2' but with a different value for the 'Nozzle offset X', which is 41,0 mm (distance between both syringe tips). Save all changes for future use in the 'Bioprinter' settings because the only setting that must be changed is the 'Nozzle Size' when the syringe tip is different from the previous printing jobs. Finally, select the printing settings and the respective extruder (1 or 2) and change the parameters and values, as shown in **Table S5**.

Table S5. Slicing parameters used to print all the structures presented in this work.

Parameter	Value	Parameter	Value
Initial/Layer Height	Tip Diameter	Top/Bottom Layers	0
Line/Wall Width	Tip Diameter	Infill Density	100%
Wall Thickness	Tip Diameter	Bottom Layers	0
Wall Line Count	Normally 1	Printing Temperature	0 °C
Print Thin Walls	Yes	All printing Speeds	15 mm/s
Horizontal Expansion	0 mm	Travel Speed	35 mm/s
Z Seam Alignment	Sharpest Corner	Retraction	Disabled
Seam Corner Preference	None	Cooling/Support	No
Top/Bottom Thickness	Tip Diameter	Build Plate Adhesion	None

Gcode Modifications

- **Printing with one extruder:** in this case, it is necessary to include commands so that the extruder does not collide with the Petri dish walls. The user must copy the first line of instructions from the Gcode file, which contains the coordinates of the location where the print job will start, remove the instructions for the extruder (E0 or E1), and add a Z component (for example, Z30) so that when the extruder moves to this first point, it does not collide with the Petri dish. The printer is programmed so that when it makes home, at the end of the printing job, it always goes up to Z = 20 mm, so there is no need to add new commands at the end.
- **Printing with two extruders simultaneously:** in this case, it is necessary to include the commands indicated in the previous point so that the extruders do not collide with the Petri Dish at the start of the operation. However, it is also necessary to include commands throughout the Gcode file. Whenever there is a change of extruder during printing, the user must modify the last line of coordinates and increase the value of the Z coordinate so that during the change of extruder, they do not collide with the side walls of the Petri dish. After the extruder change, the side walls of the Petri Dish. After the extruder change, the first line of coordinates should also be modified, again increasing the Z component.
- **UV Curing Commands:** as mentioned, the UV LEDs of the extruders are connected to PWM pins 6 and 11 of RAMPS v1.4 and can be switched on and off using the M221 Gcode command. To perform UV curing between layers the user must copy the coordinate lines of each layer, insert them below, remove the extruder motion commands, increase the value of Z, and finally put the M221 command whenever he wants to turn on or off each of the LEDs.

Printing Routine

- **Control Unit 1, Stepper Driver Set:** Initially, the cable that feeds the power supply, which in turn powers RAMPS v1.4, should be plugged into a 230V socket, and the switch button should be set to the ON position. The Arduino Mega containing the RAMPS v1.4 shield should be connected to the PC with Pronterface installed via a USB port. After turning on the Arduino, the Pronterface should be run, and the "connect" button should be selected to connect the printer to the interface, causing it to reboot. Before loading the G-code file, the home button must be selected to offset the three axes.
- **Control Unit 2, Temperature Control Set:** After downloading the file with the control algorithm, the user must open the header called system. h, where they must find the control variables for both extruders. **Figure S11**, represents the declaration of the set temperature variable of extruder 1, which, in this case, is identified as the left one. As seen, to print at room temperature, the user must declare the variable as 100. The code must be loaded to the Arduino Mega that controls the BTS7960 h-Bridges via a USB port. After connecting the cable that feeds the power supply that powers the H-Bridges, the switch button should be placed in the on position. In turn, the temperature of the two syringe extruders will evolve and stabilize at the desired temperature. Note that even if it is not necessary to change the Arduino code that controls the temperature, it must always be connected to a 5V source to control the H-Bridges and, in turn, the Peltier thermoelectric modules.
- **Printing Simulation:** Insert a syringe into the extruder(s) to be used during the printing process, load the G-code file with the print commands and click on print. With this method, it is possible to know in which position to place the container in which the printing will be done, for example, a petri dish, and at the same time, it is possible to offset the printing bed through the four screws on the bed. After performing this short calibration, the empty syringes should be removed, and for this purpose, the reverse button on the Pronterface should be used.
- **Printing Job:** After each extruder reaches the desired temperature, the syringes should be filled with ink and placed in the extruder drawers, which are locked with two pins. Before printing, the print flow factor must be set, and, in turn, the lead screw must be lowered until the organic solution is extruded from the blunt tip to check if it is clogged or not. Lastly, the print button must be selected, and the printing process begins.

```
25    /*********SET TEMPERATURE*******************/
26    // Print at room temperature: SetTemp_LEFT = 100;
27    float SetTemp_LEFT = 45;
28    /*****************************************/
```

Figure S11. Variable declaration that allows controlling the temperature of extruder 1 (E_1).